



NATIONAL ADVISORY COMMITTEE FOR AERONAUTICS

RESEARCH MEMORANDUM

for the

U. S. Air Force

DRAG NEAR ZERO LIFT OF A 1/7-SCALE MODEL OF  
THE CONVAIR B-58 EXTERNAL STORE AS MEASURED IN FREE  
FLIGHT BETWEEN MACH NUMBERS OF 0.8 AND 2.45

By Russell N. Hopko

SUMMARY

The zero-lift drag of a 1/7-scale model of the Convair B-58 external store was obtained at Mach numbers between 0.8 and 2.45 at corresponding Reynolds numbers per foot of  $3.5 \times 10^6$  and  $15.3 \times 10^6$ . The experimental drag data are compared with calculated values at both subsonic and supersonic speeds and show good agreement. In addition to the drag data, some static stability derivatives and damping factors were also obtained and are presented with the predicted values of these derivatives for completeness and for comparison. The static stability data were in good agreement with the predicted data, but the damping data obtained are considerably higher than the predicted values.

INTRODUCTION

At the request of the U. S. Air Force, the Langley Pilotless Aircraft Research Division has undertaken a flight-test program to determine the drag near zero lift of the Convair B-58 external store. This external store is a rocket-powered disposable bomb pod carried on the underside of the B-58 fuselage. Two 1/7-scale rocket-propelled models of the store alone were utilized to effect measurements over a Mach number range of 0.8 to 2.45. Some static and dynamic stability derivatives were also obtained from these tests and are presented. These tests were conducted at the Langley Pilotless Aircraft Research Station at Wallops Island, Va.

*Manney, H. M. (circled)*  
8-1-68

*8-2-68*  
*RNH*

~~CONFIDENTIAL~~

## SYMBOLS

$a_l$	longitudinal acceleration, ft/sec <sup>2</sup>
$a_n$	normal acceleration, ft/sec <sup>2</sup>
$a_t$	lateral acceleration, ft/sec <sup>2</sup>
$b$	span, ft
$\bar{c}$	wing mean aerodynamic chord, ft
$g$	acceleration due to gravity, ft/sec <sup>2</sup>
$C_D$	drag coefficient, $\frac{\text{Drag}}{qS}$
$C_{DB}$	base-drag coefficient, $\frac{P_o - P_b}{q} \times \frac{S_b}{S}$
$C_N = \frac{\text{Normal force}}{qS}$	
$C_Y = \frac{\text{Side force}}{qS}$	
$C_L = \frac{\text{Lift}}{qS}$	
$C_n = \frac{\text{Yawing moment}}{qSb}$	
$C_m = \frac{\text{Pitching moment}}{qS\bar{c}}$	
$C_{m_q} + C_{m_{\dot{\alpha}}}$	damping factor per radian, $\frac{dC_m}{d \frac{\dot{\theta}\bar{c}}{2V}} + \frac{dC_m}{d \frac{\dot{\alpha}\bar{c}}{2V} \frac{1}{57.3}}$
$I$	moment of inertia, slug-ft <sup>2</sup>
$M$	Mach number
$P_o$	static pressure, lb/sq ft

$p_b$	base pressure, lb/sq ft
$P$	period of the short-period oscillation, sec
$q$	dynamic pressure, lb/sq ft
$R$	Reynolds number
$S$	total wing area including body intercept, 2.857 sq ft
$S_b$	area of fuselage base, sq ft
$T_{1/2}$	time to damp to one-half amplitude, sec
$V$	velocity, ft/sec
$W$	model weight, lb
$\alpha$	angle of attack, deg
$\beta$	angle of sideslip, deg
$\gamma$	angle between instantaneous flight path and the horizontal, deg
$\theta$	angle of pitch, radians

## Subscripts:

X,Y,Z           longitudinal, lateral, and normal body axes,  
                  respectively

$$\alpha = \frac{d}{d\alpha}$$

$$\beta = \frac{d}{d\beta}$$

T               trim

## MODELS

The general arrangement of the model is shown in figure 1 and photographs of the models are shown in figure 2. Other pertinent

physical characteristics are presented in tables I, II, III, and IV. Approximately the forward 40 percent of the model was machined from steel; the aft section was machined from an aluminum casting. The tail fins were of aluminum, the canard fins of steel, and the wings were aluminum with tips of steel. Actuator fairings (see table IV) have been simulated on the wings and on the base of the vertical fin. The former is for the actuating mechanism of the ailerons of the full-scale article, the latter for the mechanism retracting the vertical fin of the full-scale article.

A smoke generator was installed to aid visual tracking. A pressure tank with a volumetric capacity of approximately 1 pint was located in the aft section of the model fuselage. Total pressure (to expel the fluid) was supplied by a tube inlet mounted on the strut at station 42. (See fig. 2.) The exhaust exits at the body base are shown in detail in figure 1. A fluid is carried in the tank and during the coasting flight of the model the expended fluid produced a vapor trail which was an aid to the visual tracking of the radar.

The model airframes were constructed by Consolidated Vultee Aircraft Corporation of Fort Worth, Texas.

## TEST PROCEDURE

### Instrumentation

The models were internally instrumented by the National Advisory Committee for Aeronautics with an eight-channel telemeter which transmitted the following information: longitudinal acceleration (two instruments); normal acceleration, transverse acceleration, total pressure (two instruments), static pressure, and base pressure. The base-pressure measurements were made by using four pressure orifices manifolded together and connected to a pressure pickup instrument. (See fig. 1.) In addition to the internal instrumentation, an SCR 584 radar unit was used to determine the space positions of flight. The velocity was obtained with a CW Doppler velocimeter and a rawinsonde provided atmospheric conditions and winds aloft velocities throughout the altitude range traversed by the models in flight.

### Propulsion

Model 1 attained a maximum Mach number of approximately 2.5 with a Nike modification 5 booster motor and model 2 attained a maximum Mach number of 1.5 with a booster using two Deacon rocket motors. Photographs of the models in launching position with their respective boosters are shown in figure 2.

## DATA REDUCTION

## Drag

Ground radar.- Drag coefficients were obtained during model flights by evaluating the following expression:

$$C_D = -\frac{W}{gqS} \left( \frac{dV}{dt} + g \sin \gamma \right)$$

where  $V$  is the velocity obtained from CW Doppler velocimeter and corrected to the tangential velocity along its flight path and also corrected for winds at altitudes traversed in flight.

Telemeter.- The longitudinal accelerometer data were used in the following equations:

$$C_D = -\frac{a_l}{g} \frac{W/S}{q}$$

A similar expression was used to evaluate normal- and side-force coefficients using normal and transverse accelerations, respectively.

The base-drag coefficient was determined from the relationship

$$C_{D_B} = \frac{p_o - p_b}{q} \times \frac{S_b}{S}$$

## Stability

A disturbance to the models occurred upon separation from their respective boosters. An analysis was made of the resulting oscillations from which the static stability and damping factors were obtained. The accelerations were measured along the body axes. The following expressions were used which are derived from the equations of motion using a stability axis system and standard NACA sign conventions:

$$C_{m\alpha} = -\frac{I'}{57.3} \left[ \frac{4\pi^2}{P^2} + A^2 \right]$$

$$C_{m\dot{q}} + C_{m\ddot{\alpha}} = \frac{4I'V}{\bar{c}} \left( -A + \frac{57.3 C_{I\alpha}}{2m'} \right)$$

where

$$I' = \frac{I_y}{qS\bar{c}}$$

$$m' = \frac{mV}{qS}$$

$$A = \frac{0.693}{T_{1/2}}$$

$$C_{n\beta} = \frac{I_z}{57.3 qSb} \frac{4\pi^2}{p^2}$$

A validation of these expressions to effect satisfactory derivatives for this type of configuration is fully described in references 1, 2, and 3.

Values of  $C_{L\alpha}$  were obtained from unpublished data by Convair for use in the aforementioned equations. (See fig. 3.)

## RESULTS AND DISCUSSION

### Drag

The Reynolds number per foot of the present tests is given in figure 4. A drag estimate was made of the configuration at zero lift. Friction drag as calculated with the use of reference 5 agreed well with the measured values of the subsonic drag. Base-pressure drag estimates of the strut base were made with the aid of reference 9, and the base-pressure data obtained from the present tests were used to determine the base drag of the fuselage. Increments in drag, pressure and base drag, calculated by using references 4 to 9 and the base drag from the present tests were added to the friction drag as calculated from reference 5 and are given in figure 5(a). The total estimated drag is given in figure 5(b) with the measured values of the drag coefficients. Good agreement exists between the measured and calculated values of the total drag coefficients. It can be seen in figure 6 that the drag data were obtained at small values of trim lift and trim side force corresponding to angles of attack and sideslip less than  $1^\circ$ .

## Stability and Damping Data

Stability and damping data were obtained from an analysis of normal and transverse oscillations which occurred upon the separation of the models from their respective boosters. These data are presented with the predicted values from unpublished data prepared by the Consolidated Vultee Aircraft Corp.

Static stability.- As a measure of static stability, the variation of aerodynamic center with Mach number is shown in figure 7 and as  $C_{n\beta}$  in figure 8. Values of  $C_{n\beta}$  as determined in the section on "Data Reduction" were transferred to a common center of gravity (c.g.) (proposed full-scale location) by the following transfer formula:

$$C_{n\beta_{\text{ref. c.g.}}} = C_{n\beta_{\text{test c.g.}}} - \frac{\bar{x}}{b} C_{y\beta}$$

where  $\bar{x}$  is the transfer distance.

Presented also in figure 8 are the predicted values of  $C_{y\beta}$  which were used in shifting the model data to a common center of gravity for comparison. Good agreement exists between the measured and the predicted values.

Damping.- The damping-in-pitch parameter  $C_{m_q} + C_{m_{\dot{\alpha}}}$  is presented in figure 9. The damping has been established for three center-of-gravity locations - 33.3, 36.1, and 37.1. The calculated values of  $C_{m_q} + C_{m_{\dot{\alpha}}}$  were greater for the more forward center-of-gravity locations. The increment of  $C_{m_q} + C_{m_{\dot{\alpha}}}$  between the center of gravity at 37.1 and 33.3 calculated by using reference 10 was added to the predicted values given by Convair in order to give the solid line of figure 9. The dotted line of figure 9 was constructed in a similar manner using the calculated values for 37.1 and 36.1. The curve for center of gravity at 37.1 calculated by using reference 10 was in close agreement with the predicted values given by Convair. No cross coupling was evident between the lateral and longitudinal modes of motion. The calculated damping is considerably less than the experimental damping. This is due in part to the increment in damping caused by the downwash resulting from  $C_{L_q}$  and  $C_{L_{\dot{\alpha}}}$  which was neglected in the estimation. A more complete discussion of these additional increments of damping due to pitching velocity  $C_{L_q}$  and the rate of change of angle of attack  $C_{L_{\dot{\alpha}}}$  are found in reference 11.

## CONCLUDING REMARKS

The zero-lift drag of the Convair B-58 external store was obtained at Mach numbers between 0.8 and 2.45 at corresponding Reynolds numbers per foot of  $3.5 \times 10^6$  and  $15.3 \times 10^6$ . The experimental drag data were compared with calculated values at both subsonic and supersonic speeds and showed good agreement.

In addition to the drag data some static stability derivatives and damping factors were also obtained. A comparison of flight data with the predictions of Convair is made which shows good agreement for the static stability data. The predicted damping is considerably less than the experimental damping. This disagreement is believed due in part to an increment in damping caused by the downwash resulting from  $C_{Lq}$  and  $C_{L\dot{\alpha}}$  which was neglected in the estimation.

Langley Aeronautical Laboratory,  
National Advisory Committee for Aeronautics,  
Langley Field, Va., July 15, 1955.

*Russell N. Hopko*  
Russell N. Hopko  
Aeronautical Research Scientist

Approved:

*Joseph A. Shortal*  
Joseph A. Shortal  
Chief of Pilotless Aircraft Research Division

mgk

## REFERENCES

1. Gillis, Clarence L., Peck, Robert F., and Vitale, A. James: Preliminary Results From a Free-Flight Investigation at Transonic and Supersonic Speeds of the Longitudinal Stability and Control Characteristics of an Airplane Configuration With a Thin Straight Wing of Aspect Ratio 3. NACA RM L9K25e, 1950.
2. Bishop, Robert C., and Lomax, Harvard: A Simplified Method for Determining From Flight Data the Rate of Change of Yawing-Moment Coefficient With Sideslip. NACA TN 1076, 1946.
3. Purser, Paul E., and Mitchell, Jesse L.: Miscellaneous Directional-Stability Data for Several Airplane-Like Configurations From Rocket-Model Tests at Transonic Speeds. NACA RM L52E06b, 1952.
4. Hart, Roger G., and Katz, Ellis R.: Flight Investigations at High-Subsonic, Transonic, and Supersonic Speeds To Determine Zero-Lift Drag of Fin-Stabilized Bodies of Revolution Having Fineness Ratios of 12.5, 8.91, and 6.04 and Varying Positions of Maximum Diameter. NACA RM L9I30, 1949.
5. Rubesin, Morris W., Maydew, Randall C., and Varga, Steven A.: An Analytical and Experimental Investigation of the Skin Friction of the Turbulent Boundary Layer on a Flat Plate at Supersonic Speeds. NACA TN 2305, 1951.
6. Love, Eugene S.: Investigations at Supersonic Speeds of 22 Triangular Wings Representing Two Airfoil Sections for Each of 11 Apex Angles. NACA RM L9D07, 1949.
7. Haskell, R. N., Griffith, B. J., and Kulakowski, L. J.: A Similarity Rule Correlation of the Supersonic Wave Drag Characteristics of Sweptback, Tapered Wing Planforms. Rep. No. FZA-063, Convair, Sept. 15, 1952.
8. Perkins, Edward W., and Jorgensen, Leland H.: Investigation of the Drag of Various Axially Symmetric Nose Shapes of Fineness Ratio 3 for Mach Numbers From 1.24 to 3.67. NACA RM A52H28, 1952.
9. Love, Eugene S.: The Base Pressure at Supersonic Speeds on Two-Dimensional Airfoils and Bodies of Revolution (With and Without Fins) Having Turbulent Boundary Layers. NACA RM L53C02, 1953.
10. Ribner, Herbert S., and Malvestuto, Frank S., Jr.: Stability Derivatives of Triangular Wings at Supersonic Speeds. NACA Rep. 908, 1948. (Supersedes NACA TN 1572.)

11. Gillis, Clarence L., and Chapman, Rowe, Jr.: Summary of Pitch-Damping Derivatives of Complete Airplane and Missile Configurations As Measured In Flight at Transonic and Supersonic Speeds. NACA RM L52K20, 1953.

TABLE I.- PHYSICAL CHARACTERISTICS

## Body:

Overall length, in. . . . .	87.858
Maximum diameter . . . . .	8.572

## Canard:

Span, in. . . . .	15.986
Total area, sq ft . . . . .	0.846
Exposed area, sq ft . . . . .	0.347
Airfoil section . . . . .	NACA 0005-64
Sweepback, leading edge, deg . . . . .	60
Sweepback, trailing edge, deg . . . . .	-10
Incidence, deg . . . . .	0
Aspect ratio . . . . .	2.096

## Wing:

Span, in. . . . .	29.386
Total area, sq ft . . . . .	2.857
Exposed area, sq ft . . . . .	1.449
Airfoil section . . . . .	NACA 0004.5-64
Sweepback, leading edge, deg . . . . .	60
Sweepback, trailing edge, deg . . . . .	-10
Incidence, deg . . . . .	0
Aspect ratio . . . . .	3.096

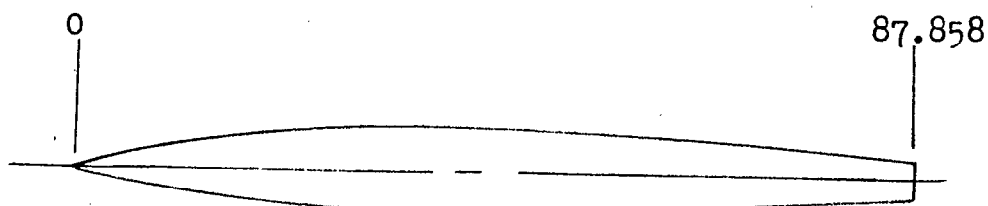
## Vertical fin:

Total area, sq ft . . . . .	0.551
Exposed area, sq ft . . . . .	0.204
Aspect ratio . . . . .	2.096
Taper ratio . . . . .	0.334
Airfoil section . . . . .	NACA 0005-64

## Vertical fin (lower):

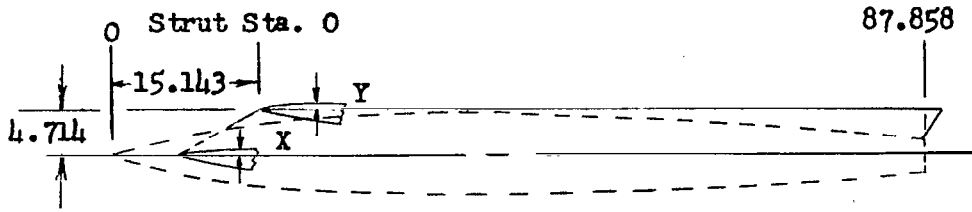
Total area, sq ft . . . . .	0.612
Exposed area, sq ft . . . . .	0.384
Aspect ratio . . . . .	1.75
Taper ratio . . . . .	0.35
Airfoil section . . . . .	NACA 0005-64

TABLE II.- POD GEOMETRY



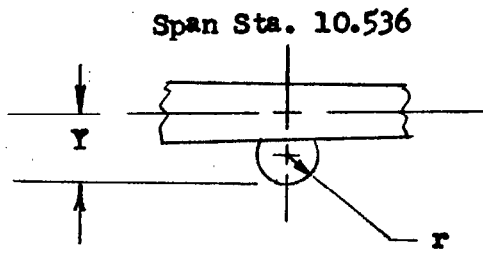
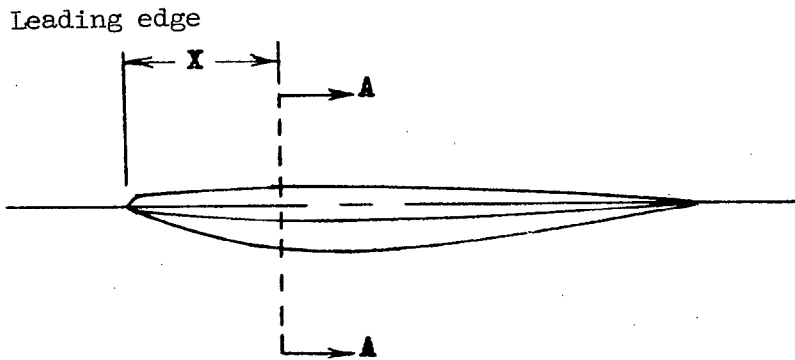
Pod station	Radius
0	0
2.286	.611
9.429	2.186
16.572	3.377
23.715	4.063
29.429	4.286
44.000	4.286
45.143	4.284
52.286	4.219
59.429	4.036
66.572	3.701
73.715	3.178
80.858	2.427
87.858	1.428

TABLE III.- POD STRUT GEOMETRY



Strut Station	Y	X
0	0	0
.214	.065	.065
.543	.109	.109
1.829	.226	.226
4.685	.409	.409
7.543	.558	.558
10.400	.688	.688
13.257	.805	.805
16.114	.912	.912
18.971	1.008	1.008
21.829	1.093	1.093
24.685	1.168	1.168
27.543	1.229	1.229
30.400	1.269	1.269
31.929	1.277	1.277
33.357	1.276	1.277
36.214	1.267	1.276
39.071	1.250	1.267
41.979	1.226	1.250
44.786	1.197	1.226
47.643	1.161	1.197
50.500	1.121	1.161
53.357	1.075	1.121
56.214	1.023	1.075
59.071	.966	1.023
61.929	.903	.966
64.786	.833	.903
67.643	.756	.833
70.500	.670	.756
73.357	.572	.670
76.214	.457	.572
79.071	.311	.457
81.357	.131	.311
81.786	.063	.131
81.929	0	0

TABLE IV.- ACTUATOR FAIRINGS



Section A - A

X	Y	r
0	0	0
1.495	.364	.170
2.697	.486	.231
3.924	.522	.248
5.152	.486	.231
6.395	.364	.170
8.626	0	0

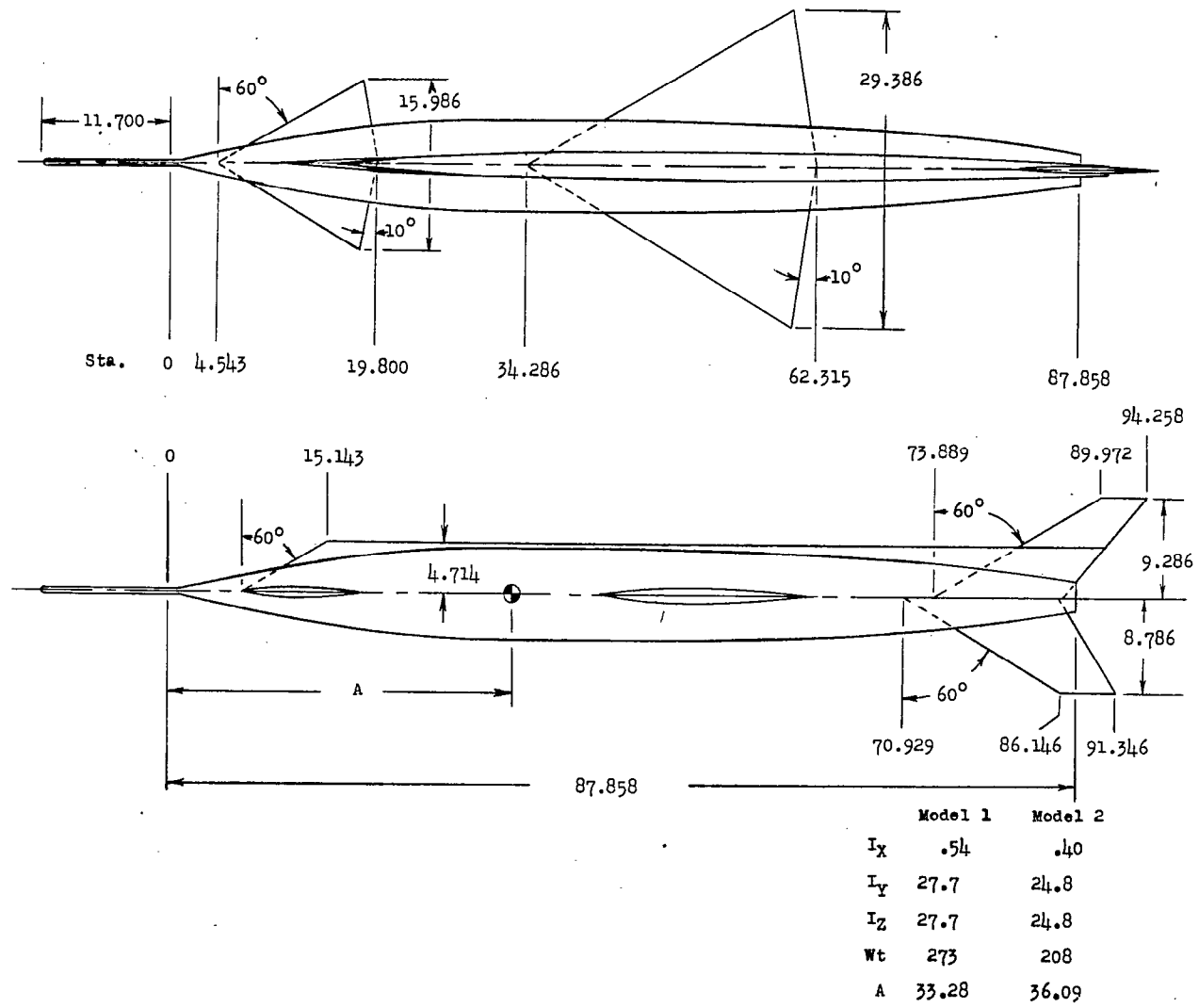
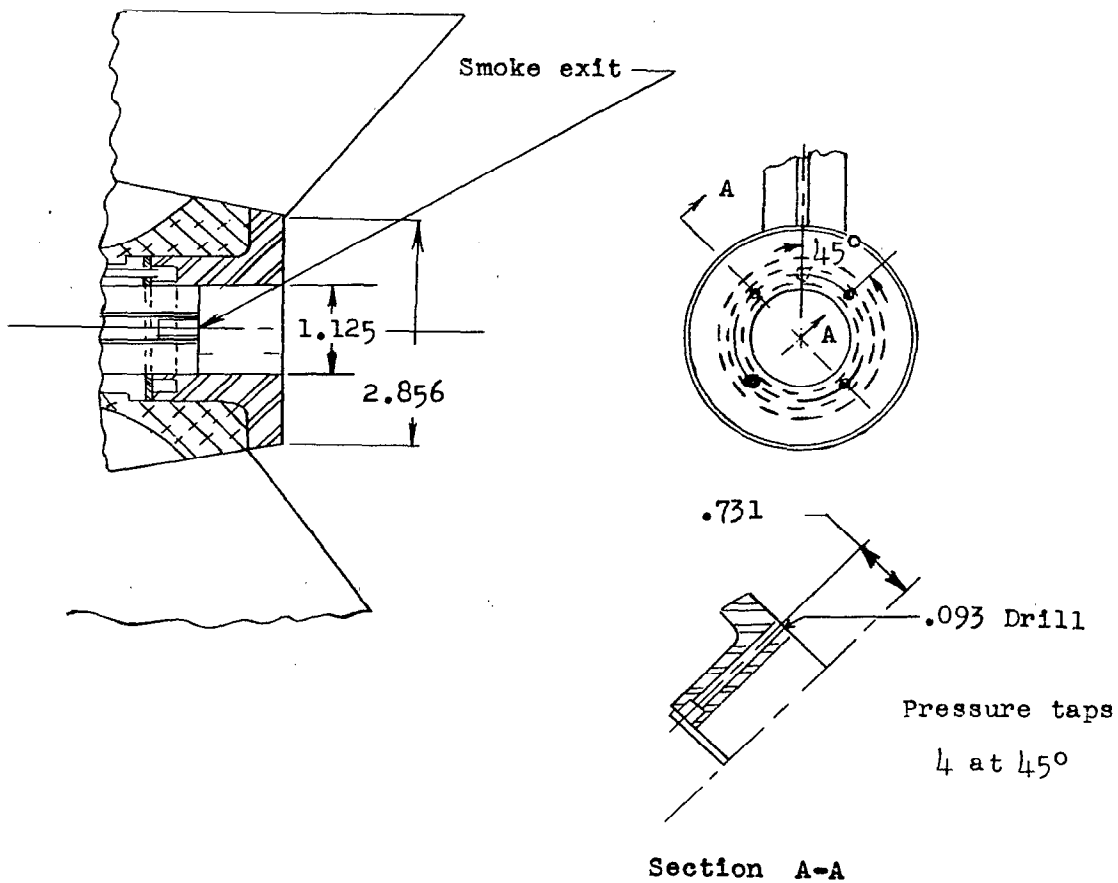
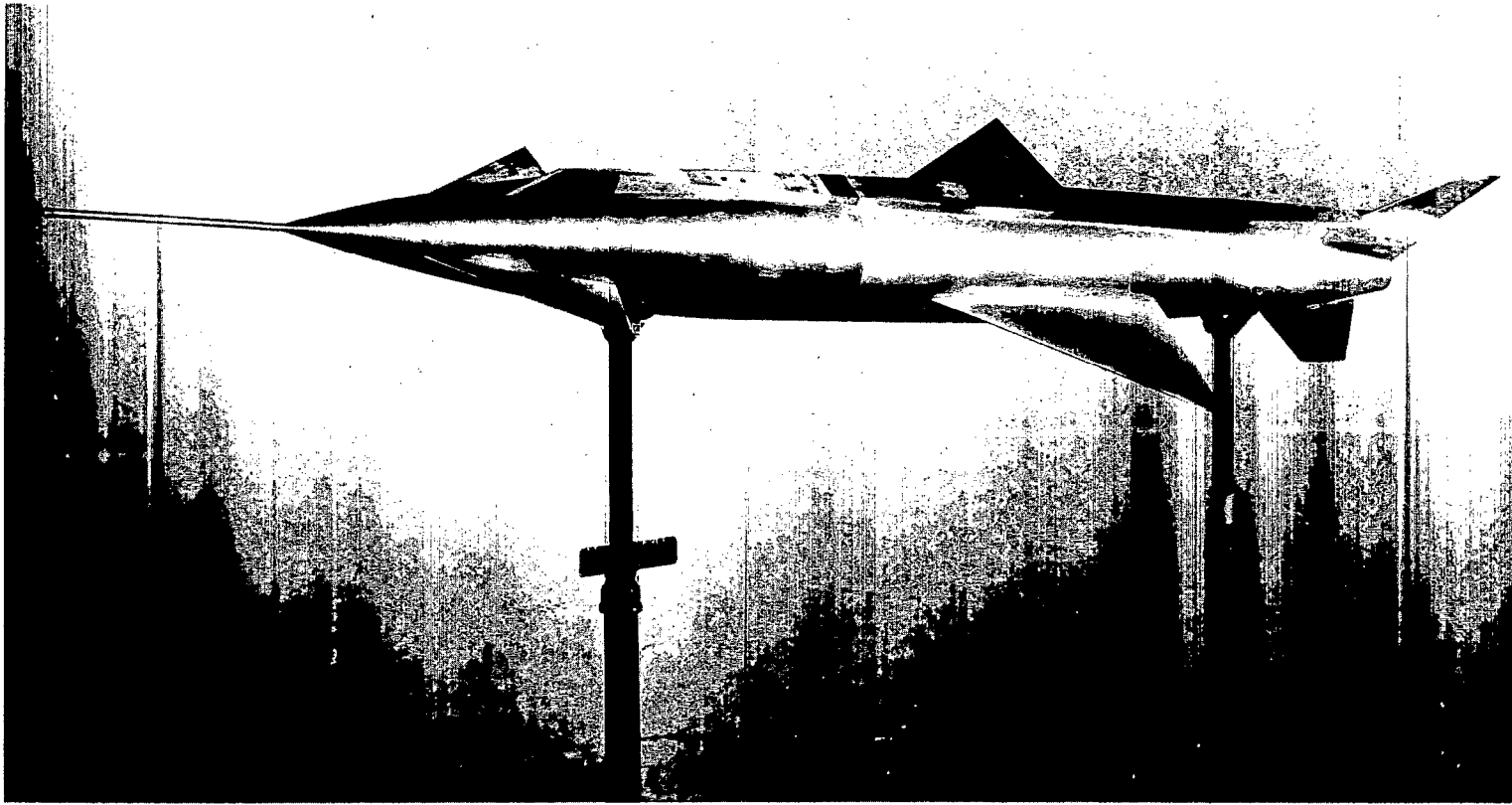


Figure 1.- General arrangement of models. All dimensions are in inches.



Detail of base

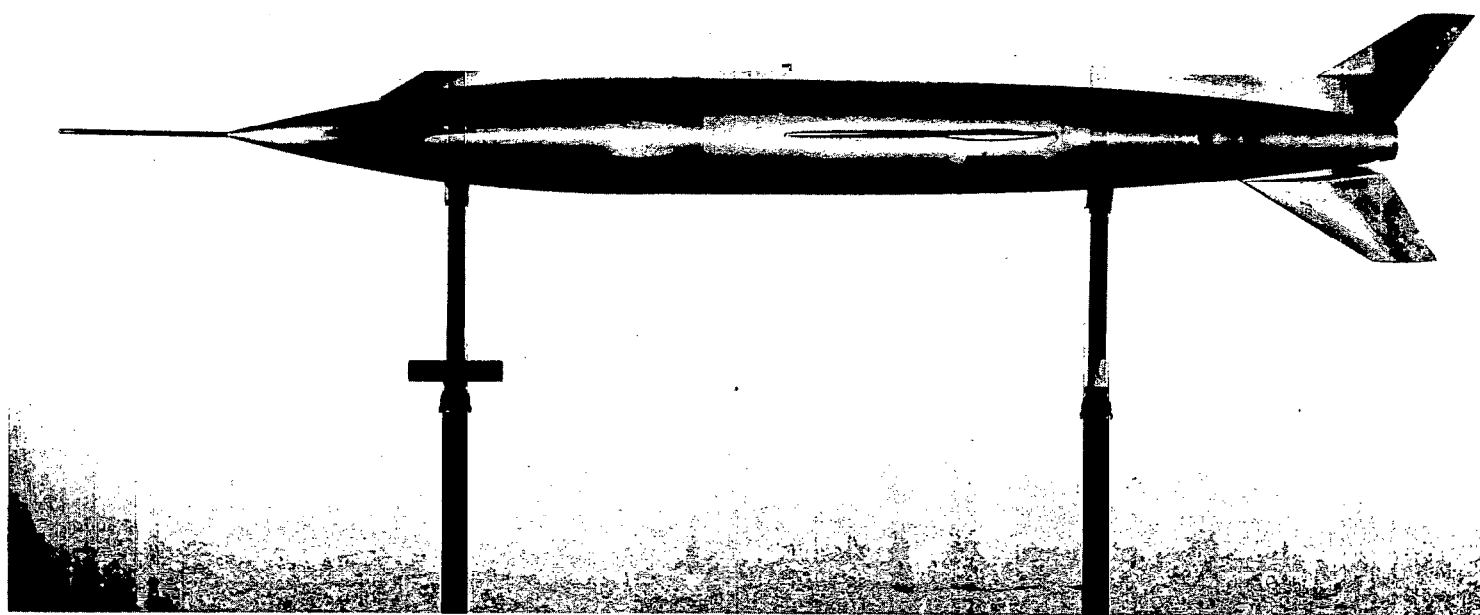
Figure 1.- Concluded.



(a) Views of model.

L-87424.1

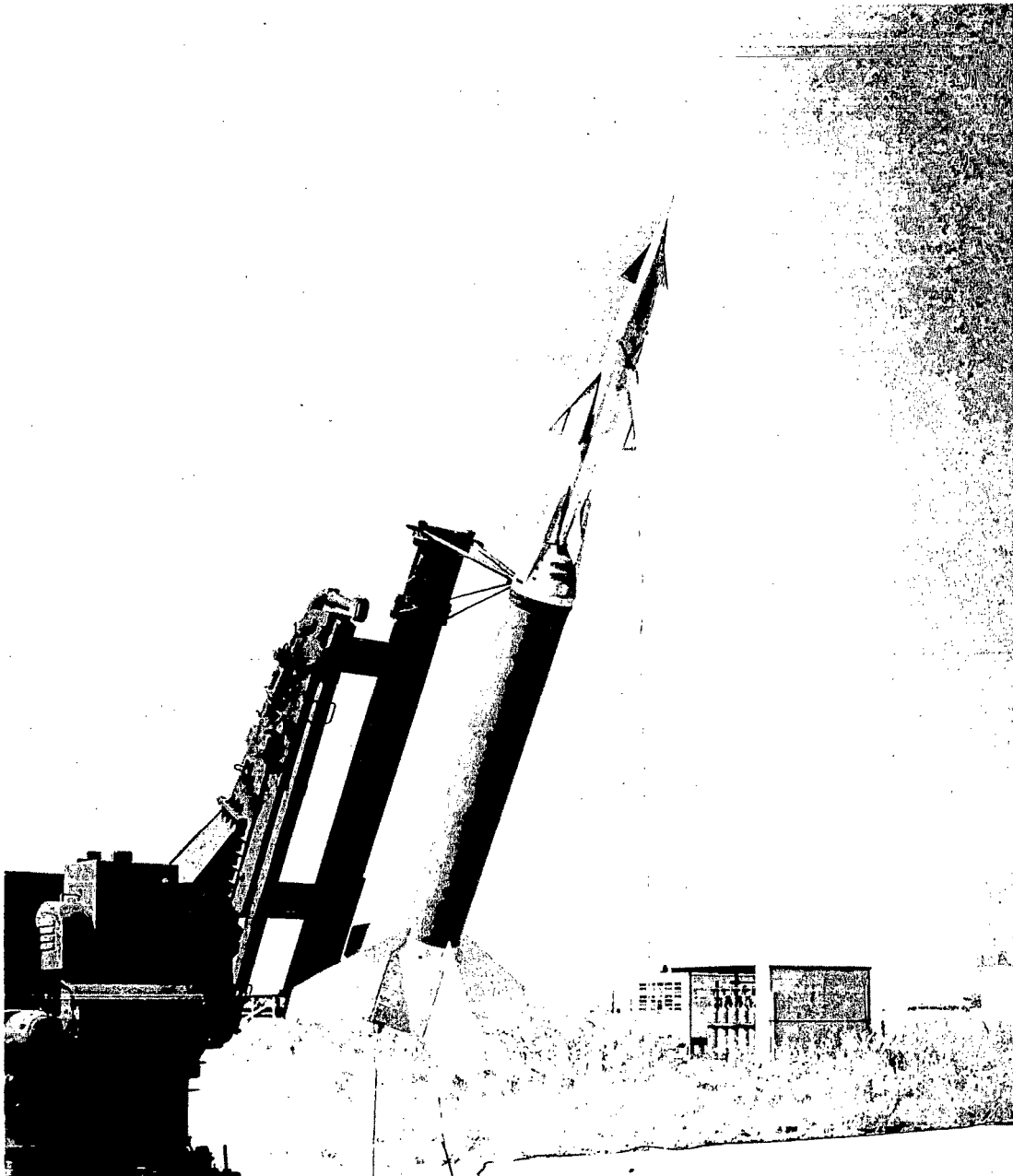
Figure 2.- Photographs of models and model booster systems.



(a) Concluded.

L-87423.1

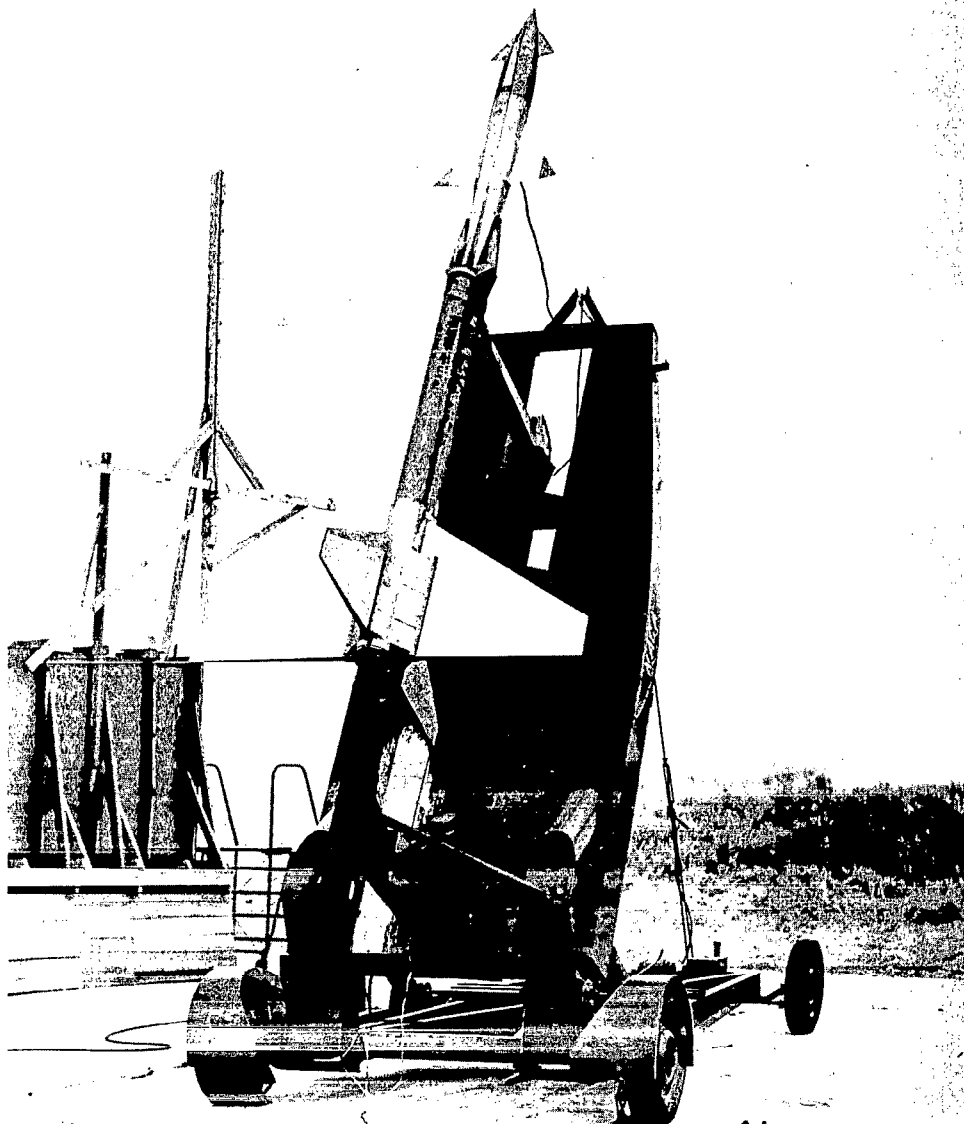
Figure 2.- Continued.



(b) Model booster systems. Model 1.

L-87018.1

Figure 2.- Continued.



(b) Concluded. Model 2.

L-87731.1

Figure 2.- Concluded.

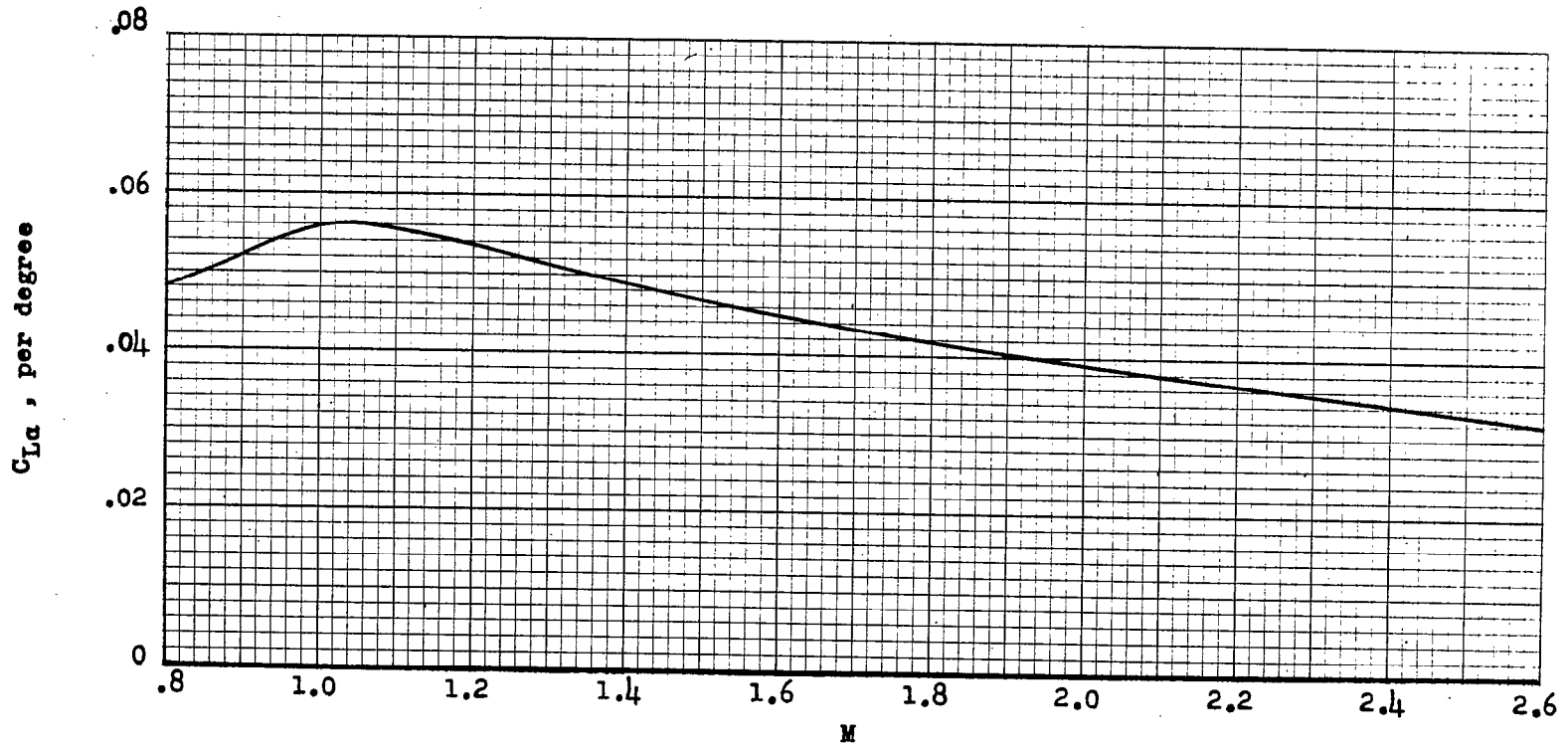


Figure 3.- Predicted lift-curve slope.

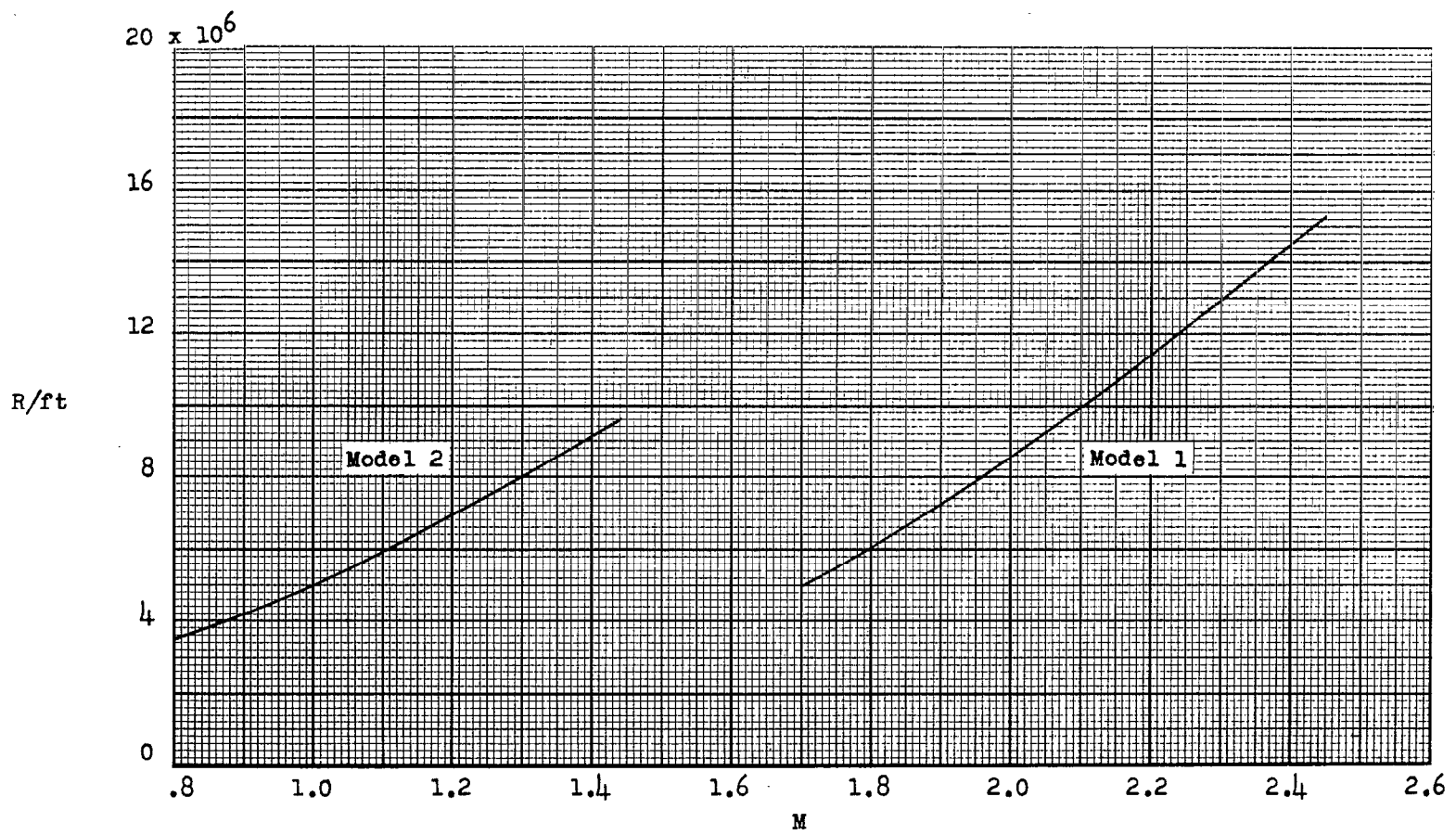
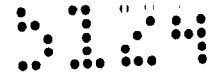
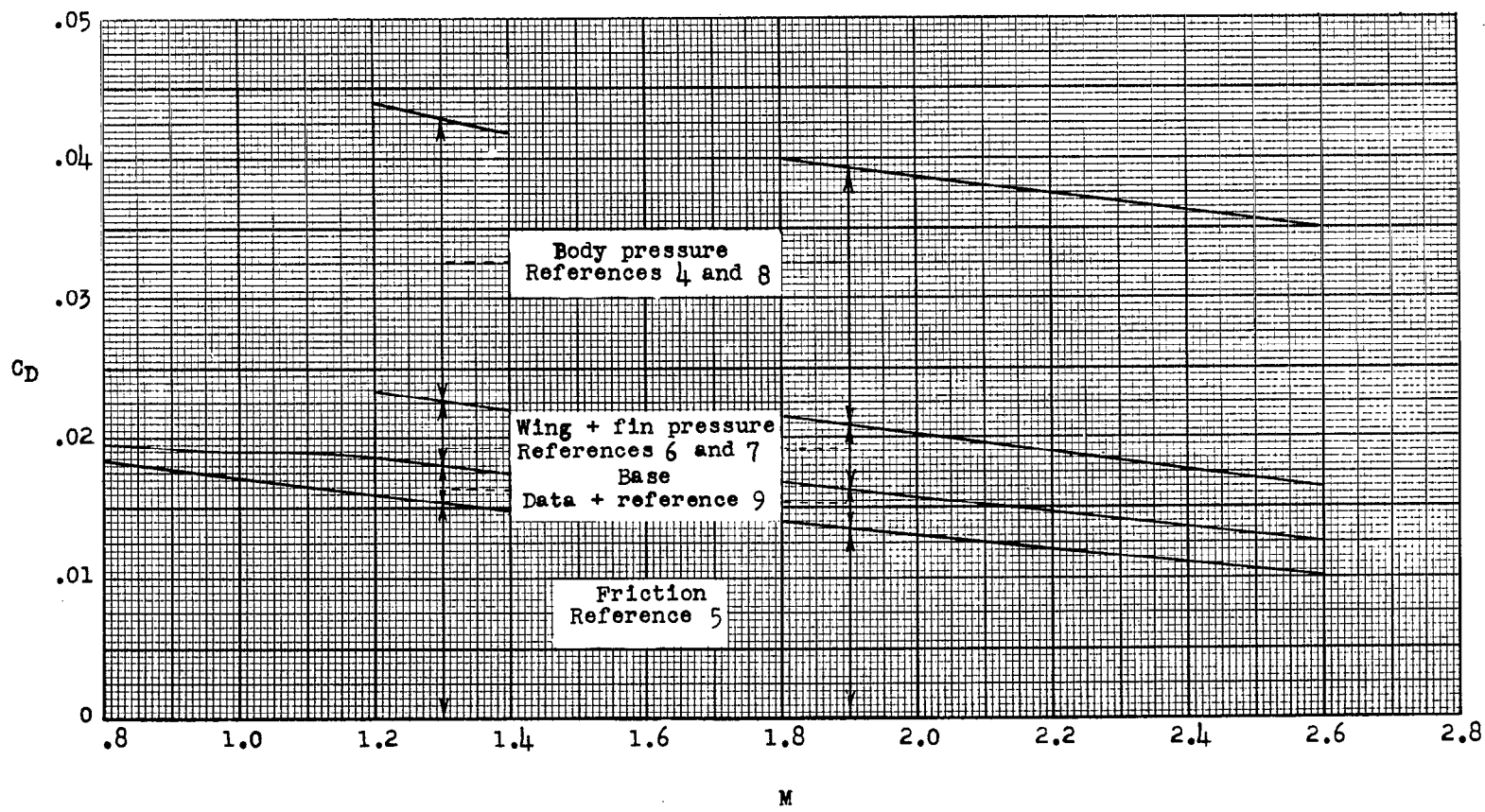
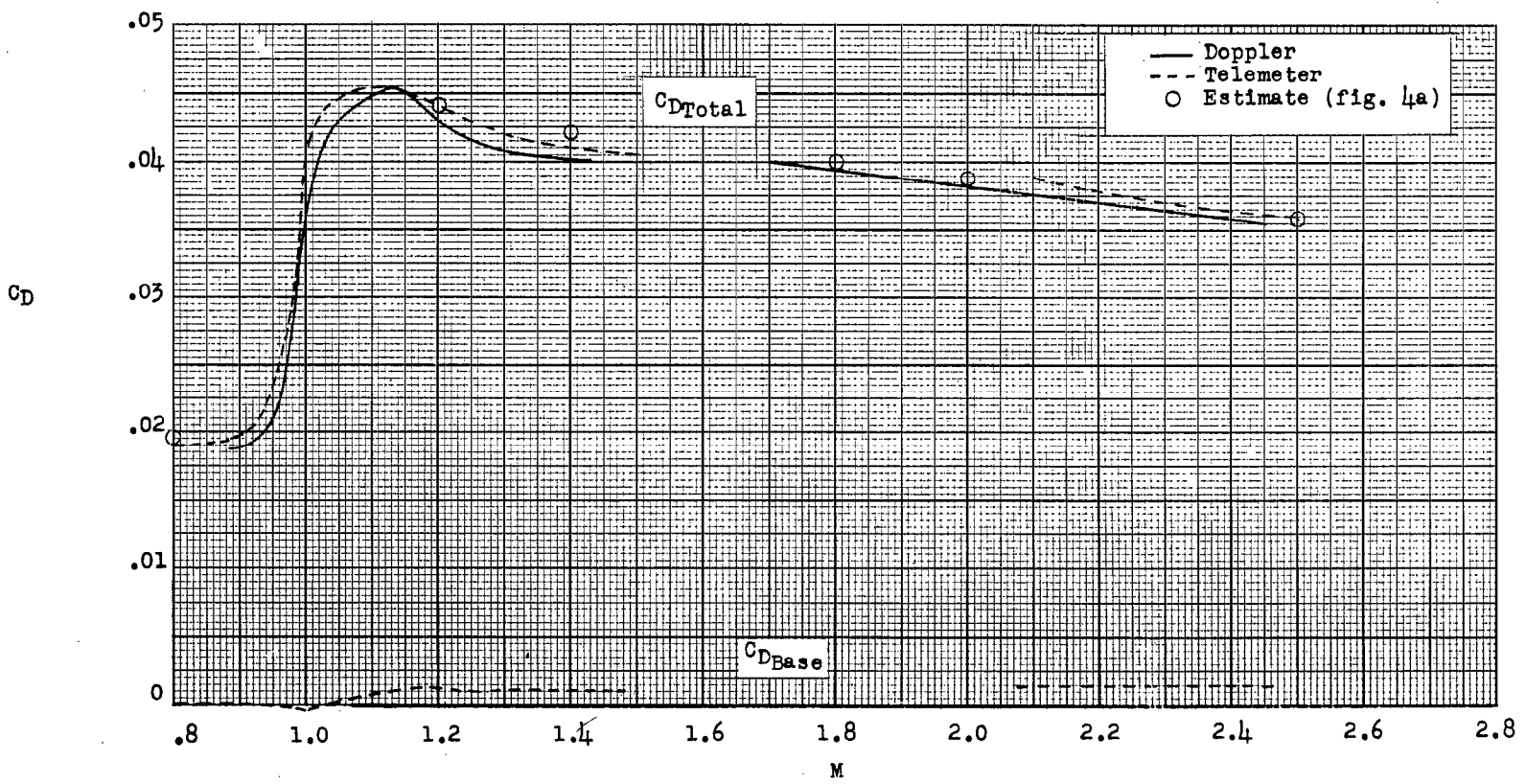
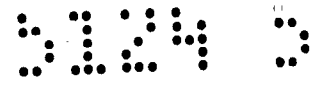


Figure 4.- Reynolds number per foot.



(a) Drag estimate.

Figure 5.- Variation of  $C_D$  with  $M$ .



(b) Drag measurements.

Figure 5.- Concluded.

524

5

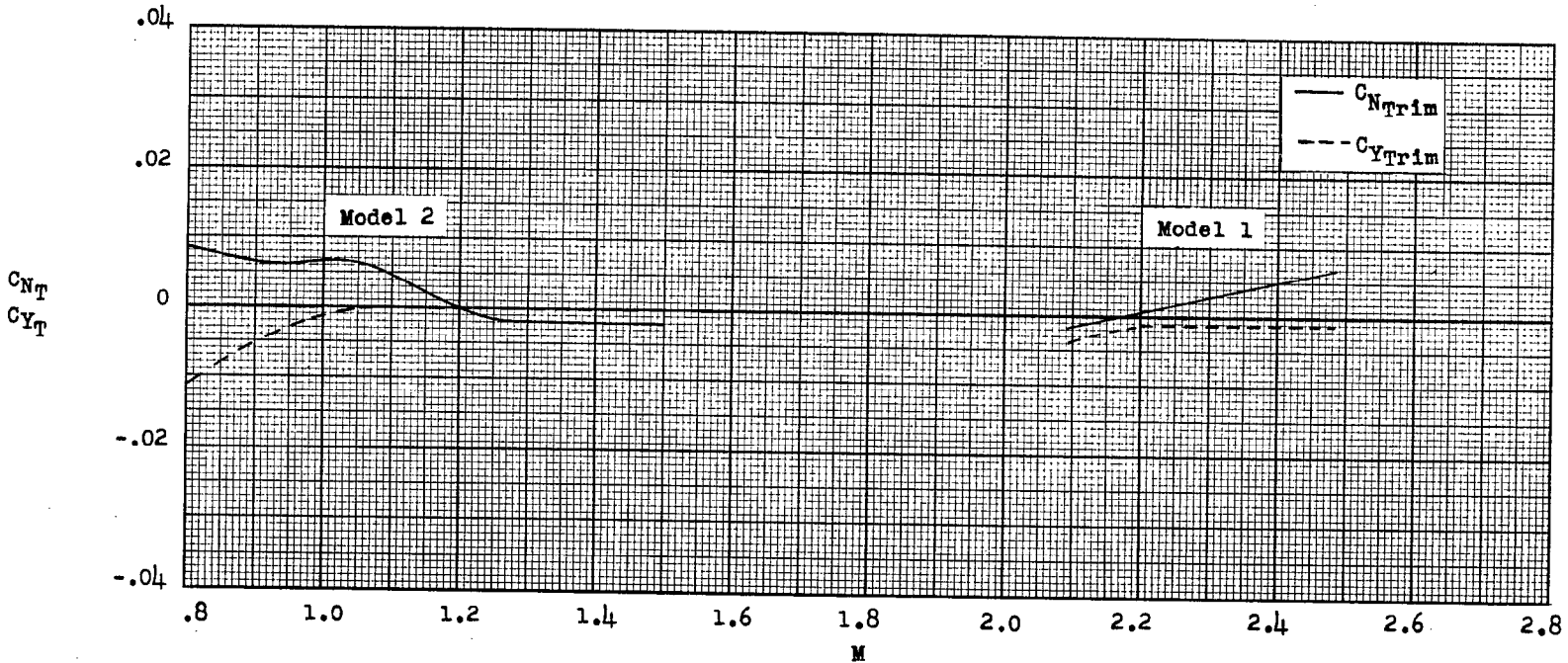


Figure 6.- Variation of trim lift and trim side-force coefficients.

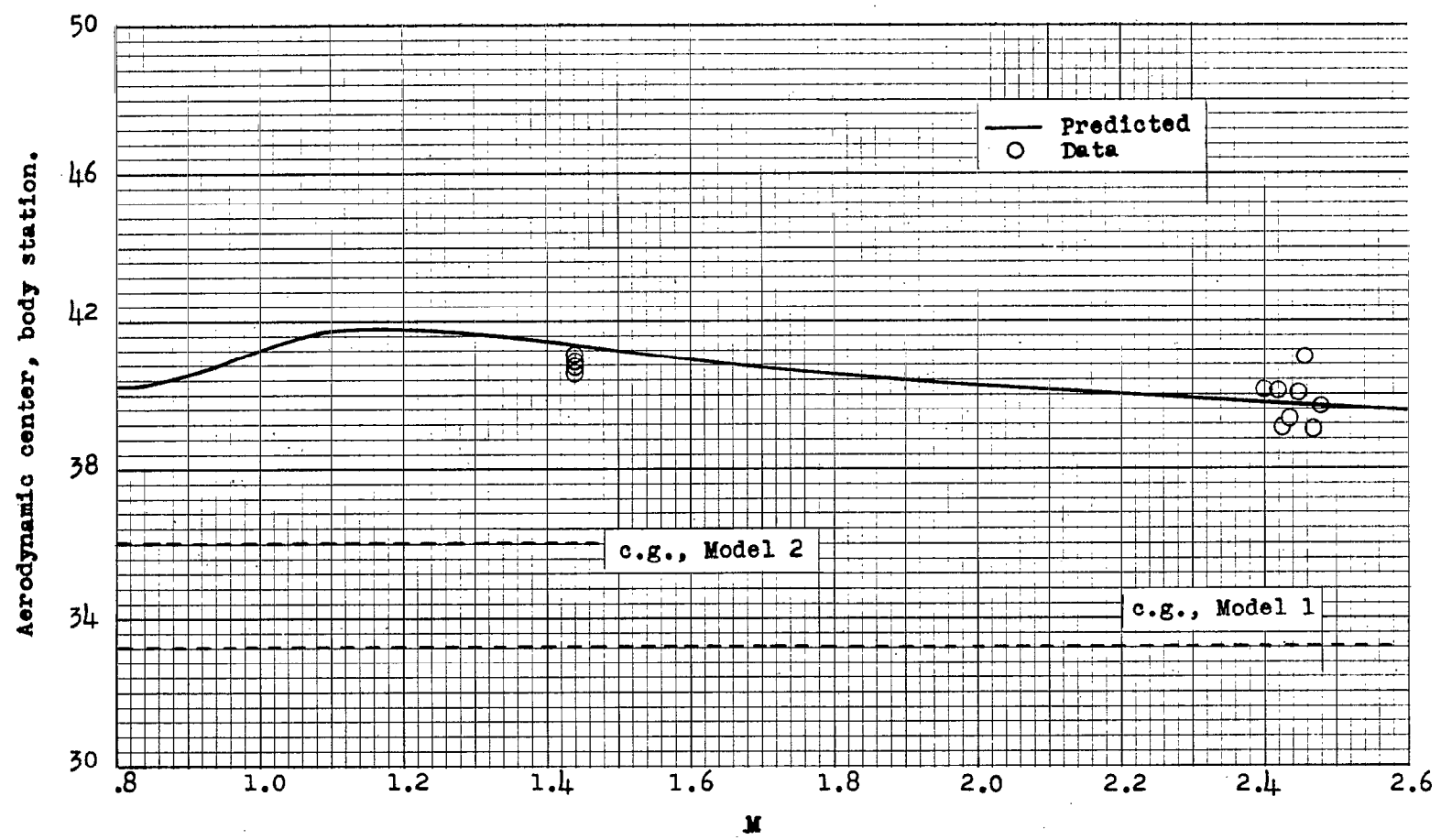
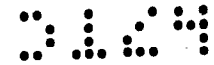


Figure 7.- Variation of aerodynamic center with Mach number.

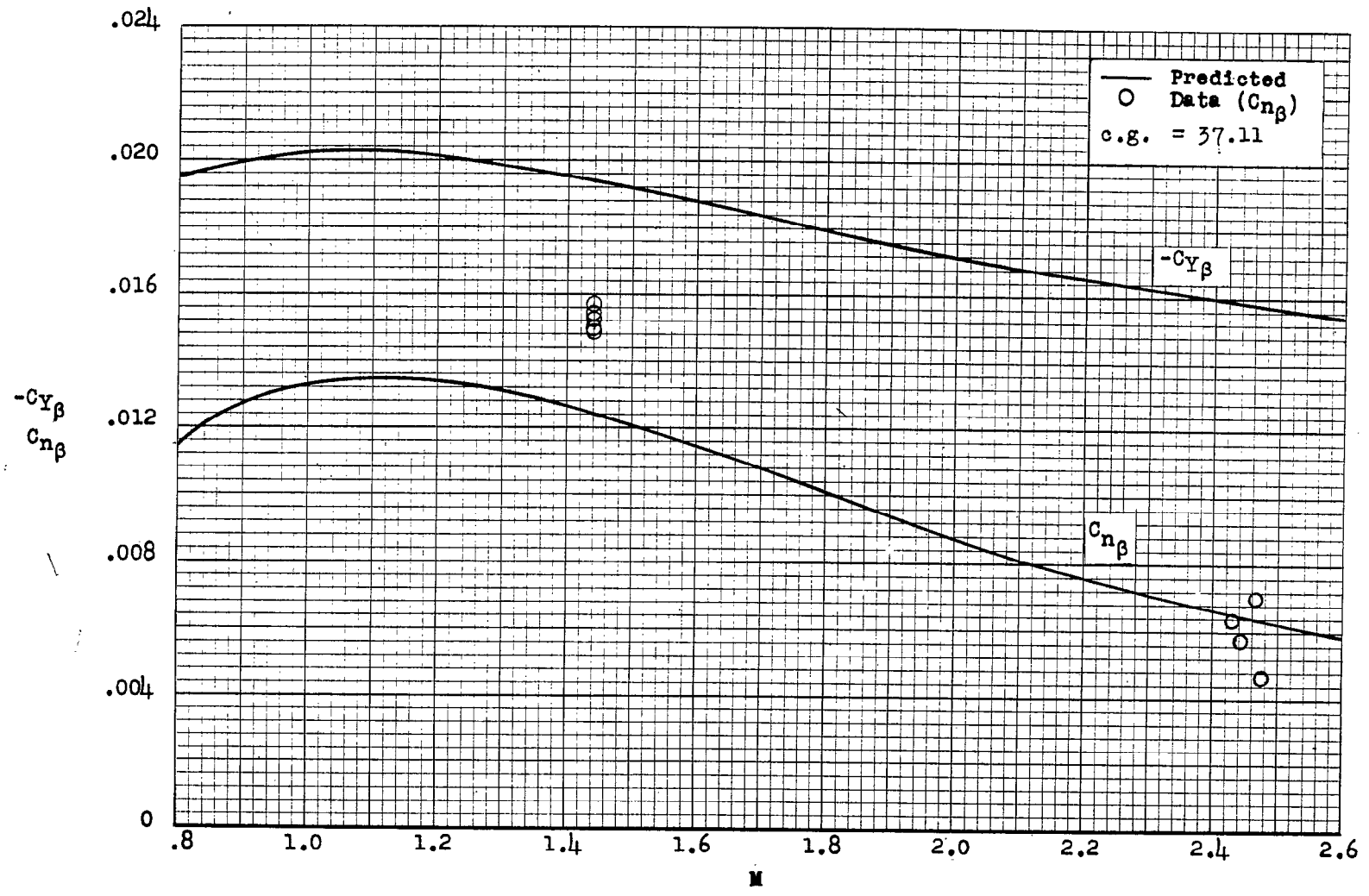


Figure 8.- Variation of side force and yawing moment with Mach number.

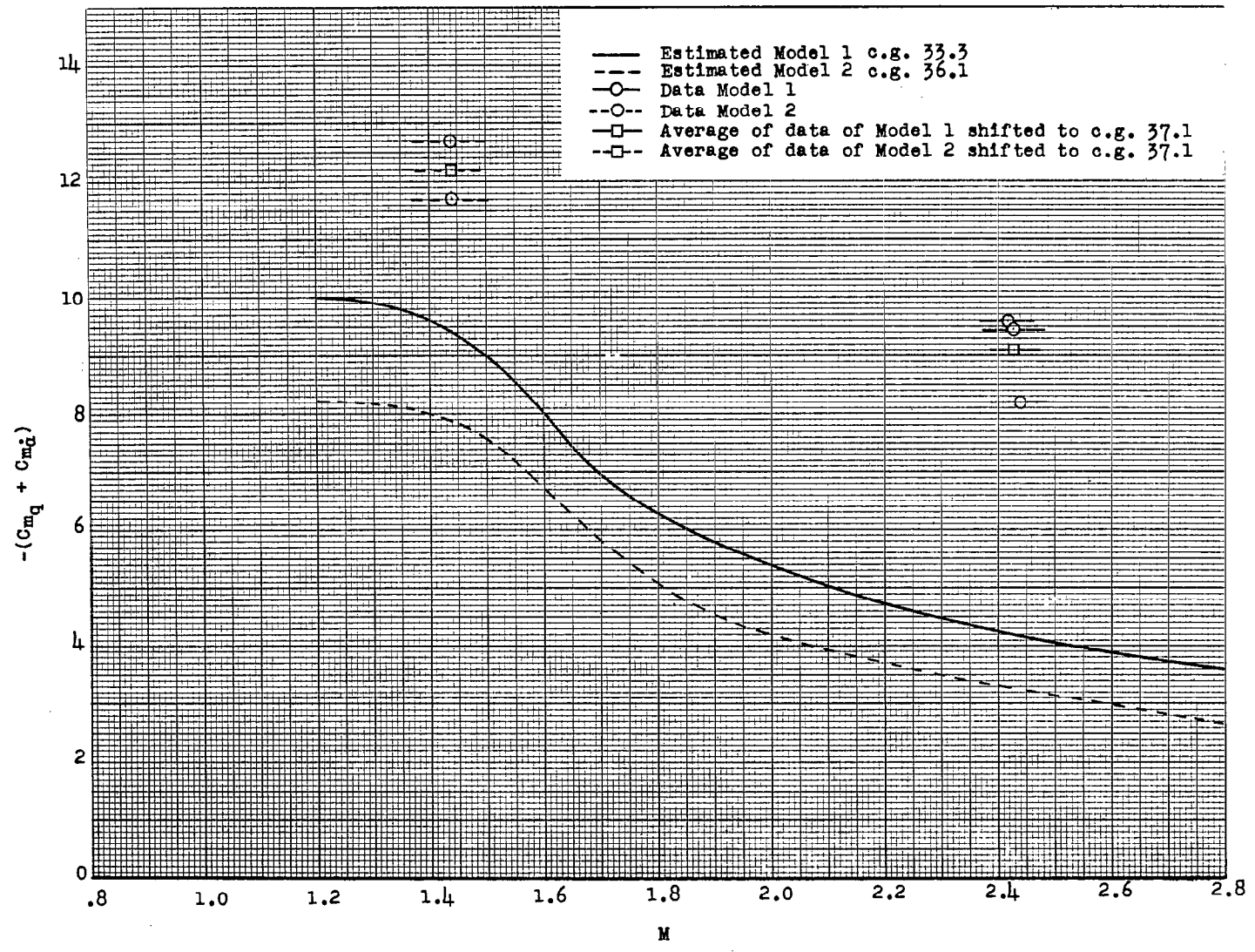


Figure 9.- Damping in pitch parameter.



~~CONFIDENTIAL~~